مجلة جامعة بابل / العلوم الصرفة والتطبيقية / العدد (1) / المجلد (17) : 2009

Modeling and Simulation of the Speed Control System for Al-Hilla Gas Turbine Power Station

Saba Yassoub Ahmed
University of Babylon, College of Engineering

Abstract

The presented work is a case study for the speed control system of the gas turbine used in Al-Hilla electrical power station. It is based on the manufacturer data given by the turbine manuals and also on the readings taken from the daily operation sheets of the power generating unit. The turbine control system is composed of three main loops: start up, temperature control, and speed control loops. A general study for the start up and temperature control loops were performed, then a detailed study for the speed control system with estimation of the system parameters was followed. The system block diagram was constructed and it turned to be a third order system with two nonlinearities, dead zone and saturation. A digital model was then developed to estimate this system in both linear and non-linear cases, where the modified Euler method was used as the numerical integration routine within the system model. An analytical solution for the control system in its linear form was also performed and the accuracy of the digital model was checked against the exact solution of the linear system transfer function. The digital model was used to adjust the value of one of the system parameters, which was not given in the manufacturer's data, in order to achieve some performance specifications. The system model was also used to study the effects of small parameters variations on the performance of the turbine control system.

الخلاصة

تضمن البحث دراسة لجهاز السيطرة على سرعة التوربين الغازي المستخدم في محطة الحلة الغازية، معتمـدا علـى المعلومـات المتوفرة من الدليل الخاص بالتوربينات الغازية وكذلك من بيانات التشغيل اليومية الخاصة بالوحدات التوربينية. يتألف جهـاز الـسيطرة فـي التوربين الغازي من ثلاثة أجزاء رئيسة هي: السيطرة على بدء الحركة والسيطرة على درجة الحرارة والسيطرة على السرعة. وقد تم إجـراء دراسة عامة على جهازي السيطرة على بدء الحركة والسيطرة على درجة الحرارة، كما تم إجراء دراسة تفصيلية على جهاز الـسيطرة علـى السرعة مع حساب المتغيرات الخاصة به فضلا عن تكوين المخطط التفصيلي لأجزاء النظام مبينا فيه درجة المعادلة التفاضلية التي تمثل النظام وأيضا أجزاء النظام ذات الخواص غير الخطية. وقد تم إعداد نموذج رقمي لتمثيل نظام السيطرة على السرعة باستخدام الحاسبة الالكترونيـة لكل من الحالة الخطية المثالية والحالة غير الخطية الفعلية، معتمدا على طريقة اويلر المعدلة في حل التكامل العددي الموجود في النظام، وقد تم إجراء دراسة تحليله لنظام السيطرة في كل من الحالة الخطية وغير الخطية. استخدم النموذج الرقمي في تحديد قيمة إحدى متغيـرات النظـام غير المتوفرة في المعلومات الخاصة بالتوربينات وكذلك في دراسة تأثير الزيادة والنقص الطفيف في قيم المتغيرات على خواص نظام السيطرة على سرعة التوربين الغازي.

List of Symbol

Symbol	Description
A	Cylinder cross sectional area (mm2)
A_1	Cross sectional area of piston (926 mm^2)
B	Damping coefficient (N.m.sec/rad)
E(s)	Error voltage (volt)
FPS	Fuel pump speed (r.p.m)
J_t	Total rotating inertia (N.m.sec^2/rad)
k	Constant, function of the hot gas characteristic and the machine
K	Constant (m^3/sec/volt)
K_1	$P_3P_{33}P_5P_2P_6P_8T_m$
N	Number of pistons =10
N_g	Generator speed =3000 r.p.m
P_5	Constant (volt/mm)
P_7	P_{77}*N where N is the gear ratio between the turbine and the fuel pump which is=1800/5100=0.353
P_{cd}	Compressor discharge pressure (bar)
P_x	Parametric pressure (bar)
Q(s)	Flow rate of hydraulic oil (m^3/sec)
R_f/R	P_3 (variable gain)
So	Rotating speed (rad/sec)
T_x	Turbine exhaust temperature ^oC
V_1	FSNL (negative voltage) volt
V_2	DSP(negative signal) volt
V_3	100% speed (negative signal)volt
V_4	Actual speed (positive signal)volt
VD(s)	Total LVDT(volt)
V_o	VCE
Y(s)	Hydraulic cylinder stroke(mm)

Sp_{rat}	Rated pump speed=1800 r.p.m
ST	Variables stroke (mm)
T(t)	Driving torque (N.m)
T_f	Turbine inlet temperature ^oC
T_{lg}	Load torque (N.m)
$T_{lt}(t)$	Load torque (N.m)
Tm	$1/J_t$

1-Introduction

The problem of controlling the turbine speed is one of the main aspects in the design and function of gas turbine power generating unit not only because the turbine speed is a major factor which affects the operation and the working of the other unit components, but also it affects the stability and the frequency of the electrical network itself. In this research an attempt is made to analyze such control system into the main components in order to understand the function and the interrelation between these components. Then use this knowledge in constructing a complete block diagram and in developing a computer model to simulate this system. Such model can be very useful in studying the reasons for any fault or malfunction which may occur during the operation. During the progress of this work, two main difficulties were faced. The first one was the restriction in doing any experimental work in the actual control system during its operation. It was forbidden for security reasons, to do any test on the generating unit or to connect any apparatus to its component while it is working. So, we had to be contented with the daily data given in the operation sheets and with the manufacturer data given in the unit manual. The second difficulty was the lack of reference on the same topic, most of the published articles on similar systems were rather interested in general description of the system then doing any mathematical study. The vast advance made in the design and use of gas turbine during the last six decades has been remarkable. The engines have been improved tremendously in terms of power, weight, efficiency and cost. They are applied successfully as ground units and for many other purposes. The electronic control of the gas turbine engine is exercised by means of a single pilot lever which controls the engine from start-up through idling to maximum speed and hence through the reheat range the pilot's lever selects the speed datum which is compared with the actual speed. If the loop is in operation then the presence of a speed error will rotate the throttle motor and hence adjusts the fuel to the engine to reduce the speed error to zero. Although the paper is particularly concerned with electronic control, it has not been setup to prove that all electronic systems should always be used in preference to the hydro-mechanical equivalent (Sadlery and Tweedy, 1963). The advancement in control technology was also discussed by (Abraham, 1969) and shows how these advancements can affect both design and application of gas turbine and compared the mechanical governor with the electrical governor and then discussed the basic types of control for the electronic control system which has an output directly connected to the fuel control valve, and the fuel control has generally fallen into one of four categories, control of burner pressure, control of spill flow, variation of displacement of fuel pump and volumetric flow control and also discussed the variation of typical fuel schedule versus compressor discharge pressure, and the fuel flow and inlet turbine temperature versus speed schedule. The control system required for the application of gas turbine to fully automatic generating station is described by (McArther and Charles, 1969), the electronic governor system is used in conjunction with a liquid fuel unit. They also discussed the various types of controls which are applied to the overall system such as governor system, speed-load control, voltage regulator; main control panel and sequence control for start-up and shut down. The fuel control system in two shaft gas turbine with heat exchanger. The supply of fuel to the combustion system is controlled by an electricity signaled proportional metering valve. The sensing of turbine inlet temperature is achieved by chromel/alumel thermocouples as in (Dent, 1970). The function of combined power and speed control system in a case of close-cycle air gas turbine by using the elements of an isostatic controller were investigated by (Bammert and Kret, 1971). A modular concept for fuel control was used with medium size, split-shaft gas turbines in the 8000-25000 hp range. The modular system combines a number of standard components such as fuel valves, limiters, electronic circuits, shut-off and pressure regulators, etc…, as described by (Ederven, 1971). The control and protective preliminary systems were designed for the gas turbine used in high temperature gas cooled reactor power plant as described by (Openshow and Estrine, 1976). An automotive gas turbine and the tasks required from its control system were discussed by (Wolzer and Meler, 1979). They used an experimental automotive gas turbine (vw-GT150), which was a two shaft design with regenerative air preheating. It's control system consists of the electronic control unit, several sensors for speed and

temperature, and hydro mechanical system for fuel supply. The application of microprocessor to control gas turbine engine was described by (Wilson, 1979). The microprocessor can provide a total supervisory and operational capability with simplicity of control. The control system in gas turbine, which is manufactured by Brown Bovery Company was described by (Trandle, 1979), which performs the following tasks, automatic set point, start-up, speed control during no load and frequency control during house hold operation, load control, turbine inlet temperature control, revolution of the turbine speed to minimum overshoot when load is supplied, and external load control of the gas turbine in a combined with waste-heat boiler. Japan's Staff Report, 1982 described a control system which is similar to our system, which used speedtronic control Mark II. Primary control of the gas turbine is accomplished by controlling fuel flow to the combustion system, supplement by varying cycle air flow by means of changes in compressor speed or the position of variable inlet guide vanes to improve part load performance in applications involving exhaust heat recovery, fuel flow, in turn, is controlled response to the speed control system, the temperature control system, or the start-up control system, whichever of the three requires the least fuel. In (Rowen, 1992.) the temperature control loop includes the action of the inlet guide vanes (IGV). IGV are situated in the air-compressor stage of the gas turbine. The role of the latter is to regulate the mass flow of air drawn into the compressor. In the operation of open cycle gas turbines, IGV are controlled during the start-up of the gas turbine and its modeling can be neglected for simulations of the gas turbine response running under normal operating conditions (Rowen, 1988). (Centeno, *et. al*., 2002) have reviewed the gas turbine models for power system stability studies. The main control loops of the typical models of gas turbines used in stability studies were described. The temperature and the acceleration control loops were also described in detail and different ways to implement them were shown. Some aspects that should be taken into account when modeling the temperature and acceleration control loops were also discussed. Later, simulations show the performance of the temperature and acceleration control loops when the gas turbine experiences increasing and decreasing steps in load. To design controllers for complex non-linear systems usually involves the use of expensive computational models (Silva, *et. al.*, 2006). A non-linear thermodynamic model of a gas turbine engine is used to evaluate a selection of designs for a multivariable PI controller configuration. An approach using variable complexity modeling (VCM) is introduced to allow for more designs to be evaluated and also to speed up the design process. Response surface methodology (RSM) is a statistical technique in which smooth functions are used to model an objective function. RSM employs statistical methods to create functions, typically polynomials, to model the response or outcome of a numerical experiment in terms of several independent variables. Regression analysis is applied to fit polynomial models to this data for various control responses. These control responses models are evaluated by a multiobjective genetic algorithm to design the controller parameters. The final designs are checked using the original non-linear model. The development of a dynamic model for a single-shaft combined cycle plant and the analysis of its response to electrical load and frequency transients as was studied by (Mantzaris, and Vournas, 2007). In particular the stability of the frequency control, as well as the implications of overheat control were investigated. The model was developed in the Simulink environment of Matlab as part of an educational and research simulation package for autonomous and interconnected systems.

2- Gas Turbine Control System:

The control system used in the gas turbine units is known as "Speedtronic Control System"(Mark II). It is manufactured by Hitachi General Electric Company and it has been widely marketed in many countries. The control system consists of three major loops (Speedtronic Control System Manual, Loft, A., 1968): Start-up, Temperature, and Speed Loops. A single basic control signal known as Electronic Control Voltage (VCE) is picked out from these three system. This is accomplished by the minimum value gate which is a diode circuit situated at the output of these three systems as shown in Figure (1). The output signal with higher voltage from the two other systems service as a back-up signals. In other words, fuel control is affected by the output signal from one of the three systems: Start-up or Speed or Temperature Control, and the output signals from the other two systems stand by are alternative signals.

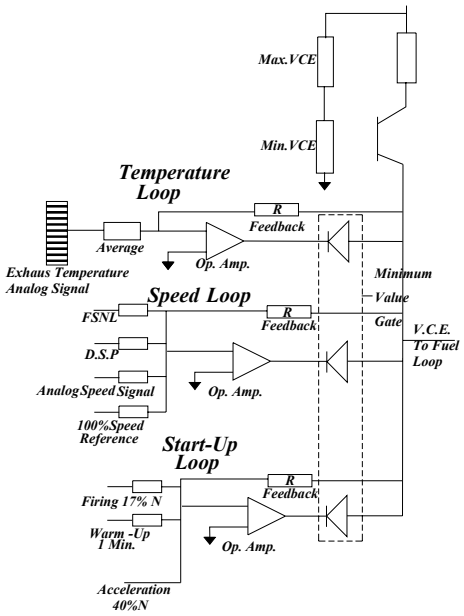

Figure (1):The Schematic Diagram for Control System.

2.1. Start-up Control System:

The start-up control regulates fuel to the gas turbine from the time when the unit starts turning (driven at the beginning by the starting device) until the turbine is on speed control. The start-up control is an open loop control. The output VCE of the VCE control loops is determined by a number of present values to set the VCE at the value of fuel flow required for firing (where VCE level is adjusted between 7-10 volts), warm-up is adjusted between 5-8 volts, so that the thermal shock to the hot gas path is diminished, acceleration VCE which is adjusted between 10-13 volts, gentle outback of fuel by the acceleration loop during the end of the start-up sequence allows for the machine to accelerate without increasing of the exhaust temperature which, on the contrary, decrease the VCE. Maximum VCE is the maximum value of the VCE that the turbine can call for when on speed governor control. The available maximum VCE is between 16-20 volts. Minimum VCE circuit on the start-up control prevents the speed or start-up amplifiers from driving VCE below the minimum value of 5 to 8 volts. This is to maintain flame in the combustors, but dose not provide sufficient energy to keep the turbine at speed as shown in Figure (2).

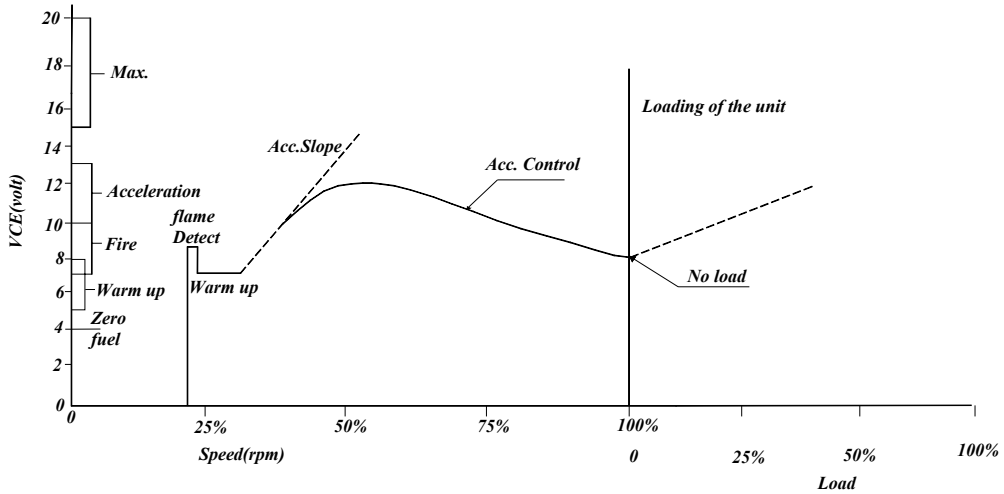

Figure(2):VCE Versus Speed in Percent During The Start-Up Sequence.

2.2. Temperature Control System:

The turbines are often operated at their maximum load capacity. Typically, this is limited by temperature in the hot gas path. For this reason, it is important to regulate fuel in order to provide an upper limit to the temperature which is encountered by the hot gas path. Turbine exhaust temperature, rather than inlet temperature, is used as the prime control parameter. The exhaust temperature is sensed by 12 fast acting thermocouples symmetrically located on the exhaust duct as shown in Figure (3). The 12 temperature control thermocouples are spaced at 30^{o} increments while the protection

thermocouples are located between these thermocouples. Then, the 12 thermocouples are averaged together to produce one signal input to millivolt/volt amplifier in order to provide D.C. output voltage which ranges from (0 to 6) volt D.C. representing, the range of control thermocouple output from 38^{o}C-705^{o}C.

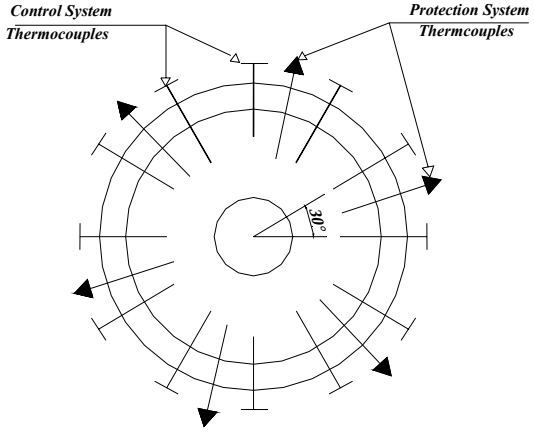

Figure(3):Thermocouple Typical Arrangement.

Exhaust temperature (T_x) measurement and its control allow to control turbine inlet temperature (T_f). For a perfect gas one would have the relation (Richard, 1981):

$$T_f = T_x \left(\frac{P_{cd}}{P_x} \right)^k \quad \ldots(1)$$

Looking at equation (1) one sees that when the pressure ratio increases due to ambient condition change, turbine exhaust temperature set point must vary on a characteristic with a given slope when the pressure ratio varies due to ambient condition changes while the turbine inlet temperature is held constant. This variation is shown in Figure(4).

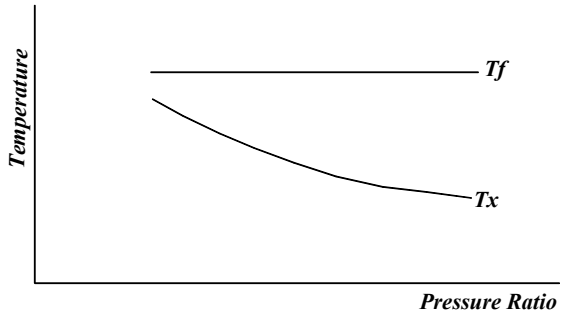

Figure(4):Exhaust Temperature (Tx) versus Pressure Ratio.

In order to examine the effect of ambient temperature on the performance of the gas turbine(Choen, et.al. 1990),let us consider Figure(5), on the hot day (50^{o}C) the air density is low, so the pressure ratio decreases. Besides, as the unit is loaded up on a hot day, it will reach the limiting firing temperature (T_f) at a high value of exhaust temperature (T_x), for this reason, the fuel consumption is at low point and the output power is also low (condition 1). On a cold day (5^{o}C), the same limiting firing will be reached at a lower exhaust temperature and high fuel consumption with high output power (condition 2).

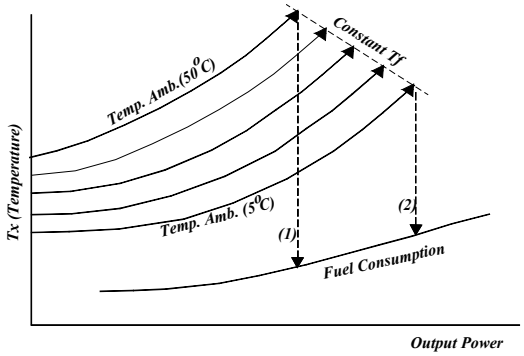

Figure (5): Performance Curve.

3. Speed Control System and its Parameters

The function of the speed control system is to provide a change in the turbine power output which is proportional, but opposite in sign, to the change in the turbine speed. This change is called the speed error and is equal to the actual speed minus the reference speed (Hogg, 1981) since the generator is normally synchronized with the power system, the speed error is also a frequency error, and speed control is used to provide frequency regulation.

3.1. Principle of Speed Control System

Gas turbine speed is detected by means of a magnetic pickup and pulses are obtained at the rate of 60pulses/revolution from a 60-teeth gear mounted on the gas turbine shaft. The pulse signal is converted to an analogue quantity proportional to its frequency, which is given as the feedback signal for speed. The analogue speed signal is summed with other speed references which are, 100% speed reference, full speed no load, digital set point, and VCE which is feedback through droop resistors to the summing junction, these signals determine how much fuel is needed by the turbine, as shown in Figure(6) of the speed control loop. When he sum of these five inputs is zero, the system is satisfied and the unit is one speed control.

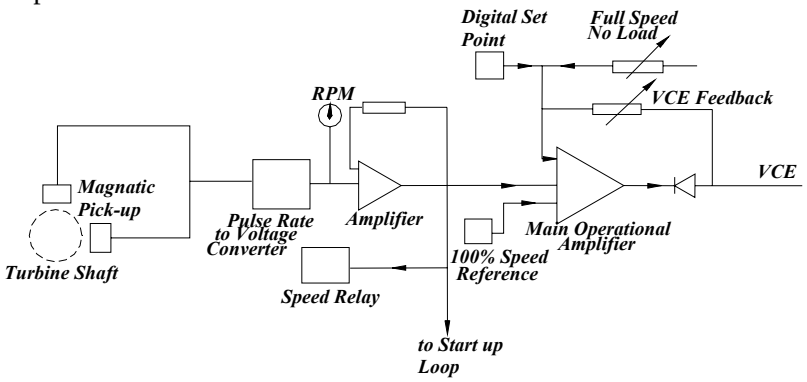

Figure (6): Speed Control System.

3.2. Components of Speed Control System:

3.2.1. Speed Inputs

(i)Speed of the unit turbine:

Speed is sensed by magnetic pick-up, which is excited by rotation of a 60 teeth wheel that is mounted on he turbine shaft. The speed signal is fed to the pulse rate analogue converter card, which is, in conjunction with an operational amplifier, generates the speedtronic analogue speed signal from (0-25volts) for speed from (0-100%). Thus the magnetic pick-up gain can be calculated:

$$P_2 = \frac{25}{5100} = 0.0049\,volt/r.p.m.$$

(ii) 100% Speed Reference Signal:

The (100%) speed reference signal is made to be exactly equal to the 100% speed analogue signal feedback to the summing junction of the speed amplifier in order to produce a basic speed error signal. It is adjusted on a potentiometer located on the "speed control card" the potentiometer gain (P_1) is also equal to 0.0049 volt/r.p.m.

(iii)Full Speed No Load (FSNL)

This signal is corresponding to no load VCE when the unit frequency matches the network frequency. FSNL voltage is inserted with other reference to provide sufficient VCE for ideal fuel for the machine. This FSNL voltage is equal 7.4 volt as given by the manufacturer.

(iv)Digital Set point (DSP):

In the speedtronic control governing characteristic, the called for speed signal is a digital set point (DSP), so called because it is elaborated by digital device before its conversion into an analogue voltage. The digital set point is sent to the summing junction of the speed/load control loop operational amplifier. It allows, through its action on VCE, to obtain the required fuel flow corresponding to the output power to be supplied. Figure(7) shows governing characteristics for DSP versus output power. The DSP appears on the ordinate axis, as a percentage of the unit speed. The output power is shown on the abscissa as a percentage of the peak load (20 MW). One sees from the first characteristic that a DSP which is corresponding to 104% speed is required to obtain 100% output power. In the control specifications, this 100% output power correspond to peak load, 50% output power would be corresponding to a DSP of 102% speed.

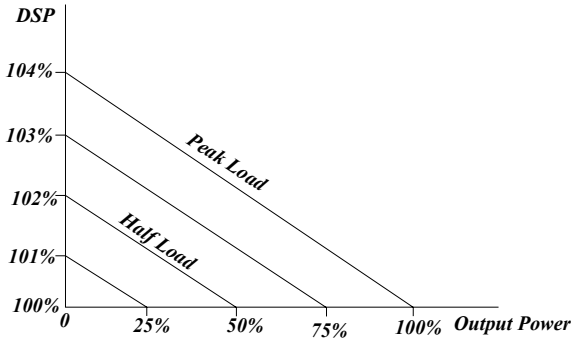

Figure(7): Governing Characteristic for The DSP vs. Output Power Relation.

The DSP circuit consists of a reversible binary counter, a digital to analogue converter, and an operational amplifier. Its function is to produce a voltage proportional to the number of counts. When the counter is empty the corresponding digital set point is 95% of the nominal speed and the voltage is such as the operational amplifier which follows will deliver -5.0 volt signal. When the counter is full the corresponding digital set point is 107% of the nominal speed and the operational amplifier will deliver +7.0 volt signal. At 100% speed, the output of the DSP is zero. The DSP gain is 1.0 volts D.C for 1% nominal speed. Figure(8) shows DSP value in volts versus its value as a percentage of the unit speed.

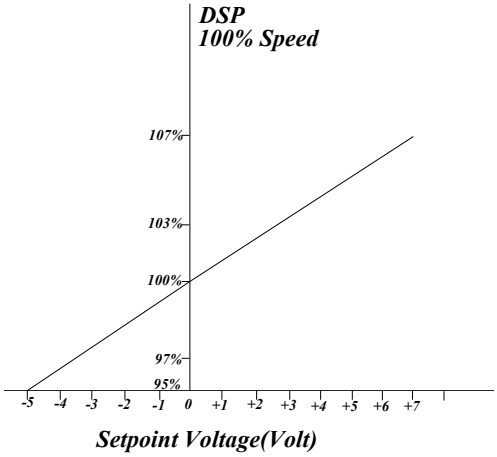

Figure(8): DSP Value in Volt and in Percent Normal Speed.

(v) VCE Feedback Signal

VCE feedback voltage signal is the output signal of the speed control loop to the fuel control system.

3.2.2. The Speed Operational Amplifier

Figure (9A) shows the schematic diagram of the operational amplifier with its five speed loop input, which is of the summing type with a variable gain factor. The input signal voltage are summed

using a separate input resistor for each signal. The various input signals are inverted and amplified by the ratio of the feedback resistor to the individual summing resistor as (Jerald, 1973, Ogata, 2005):

$$I_f = I_1 + I_2 + I_3 + I_4 \quad \ldots(2)$$

$$-\frac{V_o}{R_f} = \frac{V_1}{R_1} + \frac{V_2}{R_2} + \frac{V_3}{R_3} + \frac{V_4}{R_4} \quad \ldots(3)$$

The individual input resistors, used in the speed operational amplifier, are equal, so, we get:

$$V_o = -\frac{R_f}{R}(V_1 + V_2 + V_3 + V_4) \quad \ldots(4)$$

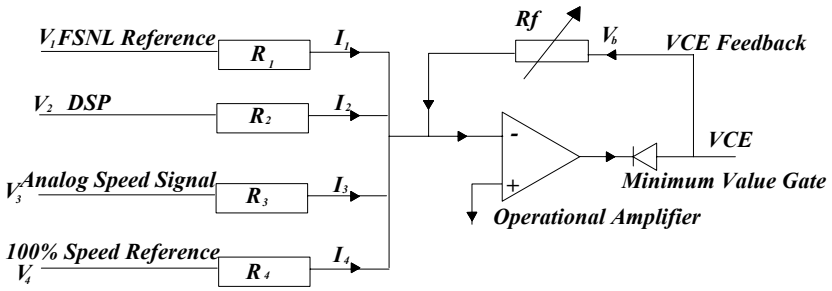

(A)

Figure (9B) shows the block diagram representation for the operation amplifier. The value of P_3 is to be adjusted according to the load condition during the actual operation of the system.

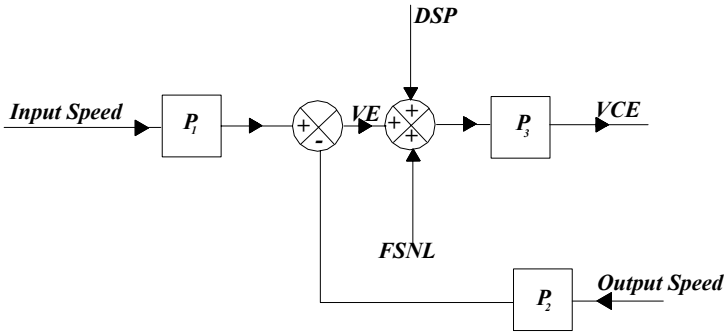

(B)

Figure(9):Show the Representation of Five Input Signals with Operational Amplifier and its Block Diagram.

3.2.3Liquid Fuel System:

The liquid fuel feed to the gas turbine is controlled by the VCE splitter's output signal LCE (Liquid Control Electronic). The VCE splitter is a device which converts the fuel control signal VCE into liquid fuel signal LCE and gas fuel signal GCE depending on which type of fuel the unit is operating. The major parts of liquid fuel control system are shown in Figure(10A) are, servo valve, the function of he servo valve is to set the stroke of the fuel pump as a function of the VCE signal and the basic components are the torque motor, the jet attached to the motor, piston, feedback spring and oil filter, hydraulic cylinder, and fuel pump. The LCE signal, after going through the servo valve card and being amplified by servo operational amplifier, actuates the electro servo valve which operates the hydraulic cylinder. This in turn varies the stroke of the fuel pump and changes the amount of fuel going to the unit.

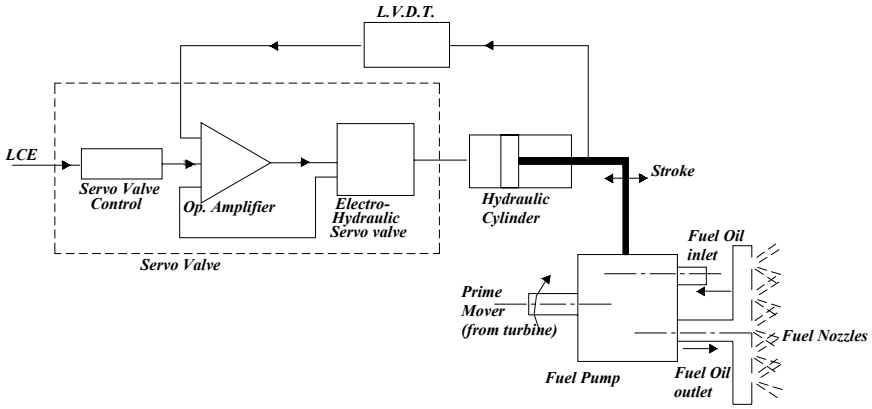

Figure(10A):Liquid Fuel Control System.

(i)Transfer function:

The transfer function which relates the error voltage signal from the operational amplifier to the flow rate of hydraulic oil can be written as (Harrison, 1969, Ogata, 2005):

$$\frac{Q(s)}{E(s)} = \frac{K}{\tau s + 1} \quad \ldots(5)$$

In hydraulic cylinder, the input is the flow rate Q(s) of oil (from the servo valve) and the output is the displacement Y(s). the transfer function for the hydraulic cylinder is ideally (Harrison, 1969):

$$\frac{Y(s)}{Q(s)} = \frac{1/A}{s} \quad \ldots(6)$$

Combination of equation (5) and (6) provides the transfer function of servo valve and hydraulic cylinder as:

$$\frac{Y(s)}{E(s)} = \frac{P_{33}}{s^2 + P_{33}\, P_{44}\, s} \quad \ldots(7)$$

(ii) Transfer Function of The Linear Variable Differential Transformer (LVDT):

The transfer function of the LVDT can be written as (Harrison, 1969):

$$\frac{VD(s)}{Y(s)} = P_5 \quad \ldots(8)$$

When assuming linear transfer function, the value of $P_5 = \frac{3.5 - 0.7}{10} = 0.28\, volt/mm$ as shown in **Figure (10B).**

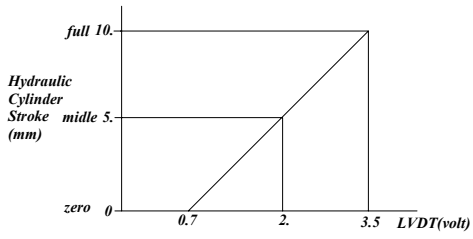

Figure(10B):Pump Stroke vs. LVDT.

(iii) Transfer Function of Servo Valve, Hydraulic Cylinder, and LVDT:

Figure(10C) shows the block diagram of servo valve, hydraulic cylinder and LVDT. The linear transfer between the output voltage (VCO) and the input voltage (VCE) is:

$$\frac{VCO(s)}{VCE(s)} = \frac{P_{33}\, P_5}{s^2 + P_{33}\, P_{44}\, s + P_{33}\, P_5} \quad \ldots(9)$$

Which can be written in the standard form as :

$$\frac{VCO(s)}{VCE(s)} = \frac{\omega_n^2}{s^2 + 2\zeta\, \omega_n\, s + \omega_n^2} \quad \ldots(10)$$

Where $\omega_n=(P_{33}P_5)^{0.5}$ =Natural frequency rad/sec. $\zeta = \frac{P_{33}P_{44}}{2(P_{33}P_5)^{0.5}}$ =Damping ratio.

Due to the lack of available data from manufacturer on these components, an optimum second order transfer function was considered to represent equation (10) with
ω_n=10.58 rad/sec and ζ=0.7 which give $\omega_n^2=(10.58)^2=P_{33}P_5$

$$\therefore P_{33} = \frac{(10.58)^2}{0.28} = 400\ rad/sec/volt/mm$$

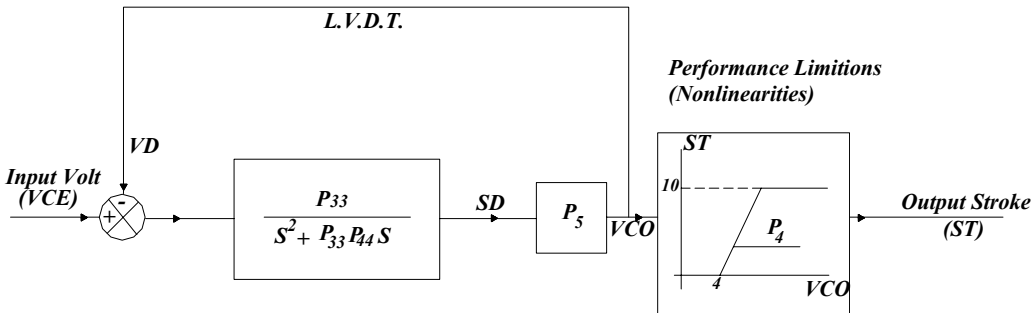

Figure(10C):Block Diagram of Electro-hydraulic Servo Valve with LVDT.

The nonlinearities exist in the system are due to the performance limitations of some of its component. Figure(11) shows the relation between the input voltage to the servo valve VCO and the output stroke of the hydraulic cylinder. It is clear that two nonlinearities are caused by this characteristic. A dead zone when VCO is less than 4 volts and saturation limit when the stroke reaches 10 mm. The voltage VCO can be obtained by multiplying the output (SD) of linear transfer function by constant P_5. In such way the dynamic and the time delay of the servo valve and the hydraulic cylinder is represented by the linear transfer function, while performance limitations are represented by these nonlinearities. The slope of this characteristic line is the parameter P_4 =0.714 mm/volt.

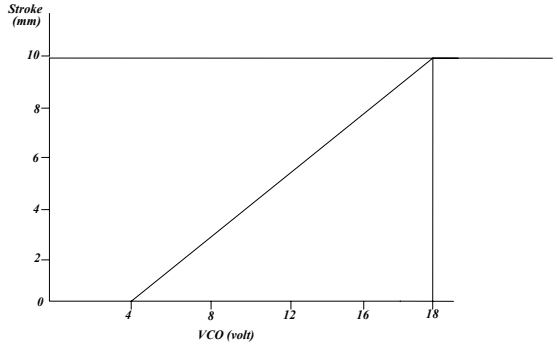

Figure(11):System Non-Linearities.

(iv)Fuel Pump

The fuel pump, used in our system, is a variable stroke pump (Piston Type). This pump is driven directly through a gear from the turbine shaft. The piston return plate or (Wobble Plate) is fixed. As the cylinder block rotates, it carries with it the pistons which bear on the Wobble Plate. This plate is positioned in such a manner that the cylinder volume is increasing as the piston passes the inlet part and decreasing as the outlet is passed. Thus the fuel which was taken in through the inlet port is expelled through the outlet port. The fuel rate of the piston pump is changing by adjusting the angle of Wobble plate which is done by the stroke of the hydraulic cylinder. This stroke is detected by LVDT and the output signal is feedback to the analogue calculator. As a result a proportional relationship is maintained constantly between the LCE signal, the pump stroke and the fuel flow rate. Since the fuel pump is driven by the turbine the fuel flow rate is also proportional to the turbine speed. A block diagram for the fuel pump is shown in Figure (12) from which the output fuel flow Q(s) can be written as (Gill, 1978, Rowen, 1983):

$$Q(s) = P_6 * ST(s) + P_{77} * FPS(s) \quad \ldots(11)$$

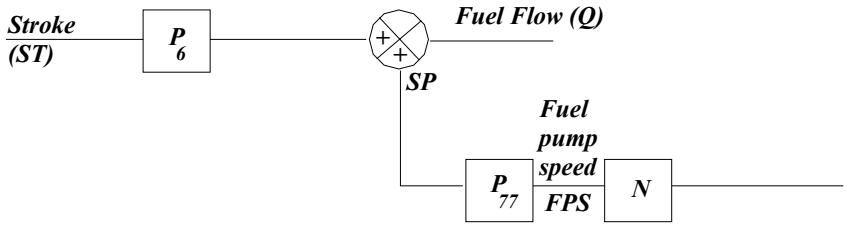

Figure(12):Block Diagram of Fuel Pump.

To find the two constants as follows:

1-When the pump is driven at a constant speed, the output flow rate Q(s) can be varied by changing the displacement which is accomplished by varying the pump stroke ST(s). Thus the fuel output from the pump is controlled by the pump stroke only. The operation characteristic for the fuel pump as given by manufacturer is shown in Figure (13) from which we notice that at zero strokes, no fuel is obtained. As the pump stroked, the output flow rate increases in linear manner. The transfer function for fuel pump is:

$$\frac{Q(s)}{ST(s)} = P_6 \quad \ldots(12)$$

When P_6 is constant, depending on the number of pistons, cross section area of piston, and pump speed and it can be calculated as:

$$P_6 = A_1 * n * Sp_{rat} \quad \ldots(13)$$

$$\therefore P_6 = 16.67\ lit/min/mm$$

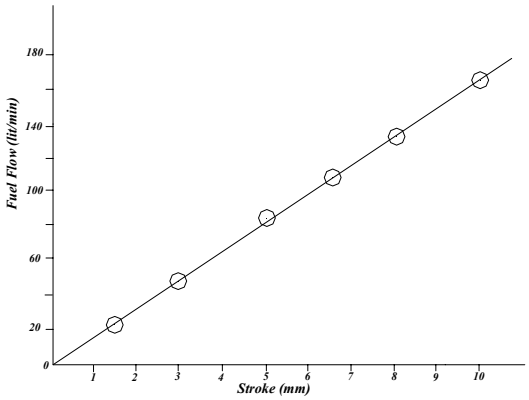

Figure(13):Pump Stroke vs. Fuel Flow.

2- When the stroke is constant at any value except zero, the output fuel flow rate can be varied by changing the pump speed. The transfer function of fuel flow rate change in pump speed can be written:

$$\frac{Q(s)}{FPS(s)} = P_{77} \quad \ldots(14)$$

When P_{77} is constant which can be calculated using the operation characteristic of Figure (13) at stroke equal 5 mm, the fuel flow is 85.15 lit/min. Applying equation (11) to get:

$$85.15 = 16.67 * 5 + P_{77} * 1800$$

Which yields

$$P_{77} = 0.001\ lit/min/rpm$$

Also, when applying this relation for different strokes we obtain nearly the same value for P_{77}. the product of this parameter by gear ratio (N) between the turbine shaft and the pump shaft is the parameter P_7 used in the system model.

3.2.4.Gas Turbine:

3.2.4.1.Fuel Power Coefficient:

The purpose of the gas turbine is to convert the energy in the supplied fuel to useful power with the turbine operating at some base speed, and assuming the change in power developed can be considered as proportional to change in fuel flow rate (δQ) (Harrison, H.I., Bollinger, J.G., 1969):

$$\delta\ outputpower = P_{88} * \delta Q \quad \ldots(15)$$

Since the power is proportional to the product of torque and speed, where speed is assumed to be basically constant, so we can write:

$$\delta T = \frac{P_{88}}{So} * \delta Q \quad \ldots(16)$$

$$\delta T = P_8 * \delta Q \quad \ldots(17)$$

Where δT is the change in developed torque, and P_8 is the appropriate proportionality factor, or gain, which would be obtained from the performance curve of the turbine. This parameter can also be obtained from the relation:

$$\eta = \frac{\delta\, outputpower}{L.C.V.* \delta Q} \quad \ldots(18)$$

Which yields

$$P_{88} = \eta * L.C.V. \quad \ldots(19)$$

Where η is the overall efficiency of gas turbine at a specific load, from the manufacturer data, the efficiency at no load is equal 8.5 %, at 1/2 base load is equal 25 %, and at maximum load is equal 28 %, as shown in Figure(14), L.C.V. is the high calorific value of gas oil, which is used in the unit, this is equal to 43100 kJ/kg, for fuel with specific weight of 946kg/m^3, thus equation (19) can be written as:

$$\therefore P_8 = \eta * 1273.176 \qquad (N.m / lit / min)$$

Using this expression we can get different values for parameter P_8 at the different loads as also shown in Figure (14).

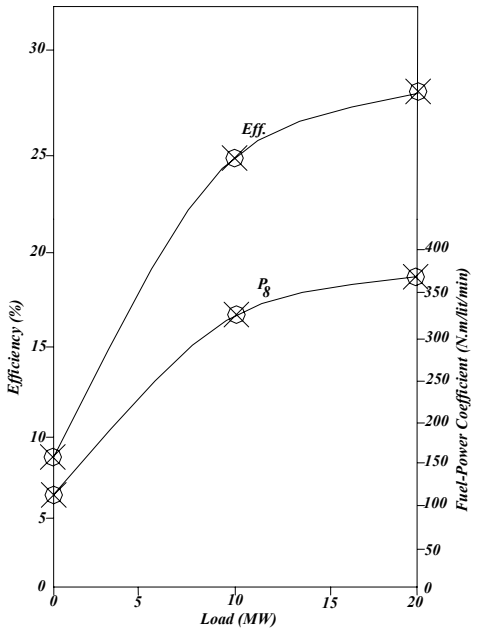

Figure(14):Fuel Power Coefficient and Thermal Cycle Efficiency Vs. The Variable Load.

3.2.4.2. Inertia and Damping:

A gas turbine will exhibit rotating inertia damping If the connection between the turbine and the driven generator is assumed to be rigid, then the turbine inertia and damping can be conveniently combined with that of the generator. Total inertia given by the manufacturer is 1340 kg.m^2, which yields, J_t=2.50 N.m.sec^2/rad, the appropriate torque equation for the turbine can be written as (Harrison, Bollinger, 1969):

$$T(t) - T_{Lt}(t) = J_t \frac{dSo(t)}{dt} + B\, So(t) \quad \ldots(20)$$

Equation (20) can be utilized for the turbine components as shown in ***Figure (15)***. The load torque can be calculated from the generator power as:

$$W = T_{Lg} * (N_g) * \frac{2\pi}{60} \quad \ldots(21a)$$

$$\therefore T_{lg} = \frac{W(MW) * 10^6}{2 * \pi * N_g / 60} = MW * 3183.1(N.m) \quad \ldots(21b)$$

The torque load when converted to turbine shaft must be multiplied by the gear ratio, as:

$$T_{Lt} = \frac{N_g}{N_t} T_{lg} \quad \ldots(22)$$

If we substitute the above equation into ***equation (21b)***, we get

$$T_{Lt} = 1873.36 * MW \,,\; T_{Lt} = P_9 * W \quad \ldots(23)$$

The damping is the dissipation of energy due to the friction in the bearings supporting rotating components. The value of total damping coefficient ***(B)*** is not given by the manufacturer, so we must calculated as follows:

At no load normal running speed of SO(5100 r.p.m) and fuel flow Q=43.4 lit/min, where P_8=108.22 N.m/lit/min, as shown in Figure(14) from equation (17) we have:

$$T = Q * P_8 = 4702.16\ N.m \quad \ldots(24)$$

Also, ***equation (20)*** yields:

$$T = B * So \quad \ldots(25)$$

Where the change in speed $\frac{dSo}{dt} = 0$, substituting ***eq,(25) into (24)*** to get:

$$B = \frac{Q * P_8}{So} = 8.8\ N.m.sec/rad$$

The value of parameters P_{10} is now calculated

$$P_{10} = B * \frac{2\pi}{60} = 0.922\ N.m/r.p.m.$$

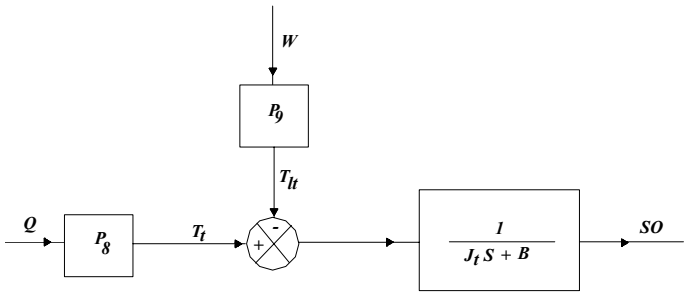

Figure (15):Block Diagram of Gas Turbine.

3.3. Complete System Block Diagram:

The complete block diagram for the gas turbine speed control system can be established as shown in Figure (16). It is clear that the system is 3rd order in linear terms, it posses two nonlinearities, dead-zone and saturation limit. This block diagram permits two types of input, a reference speed change (SI) and load disturbance (W). The parameter (P_{77}), in the system block diagram, which can be replaced by another parameter (P_7), the digital set point also related to the input load (W) by the constant (K_2), where K_2=0.2 volt/MW, which yields DSP=4 volt at load 20MW and DSP=2 volt at load 10 MW.

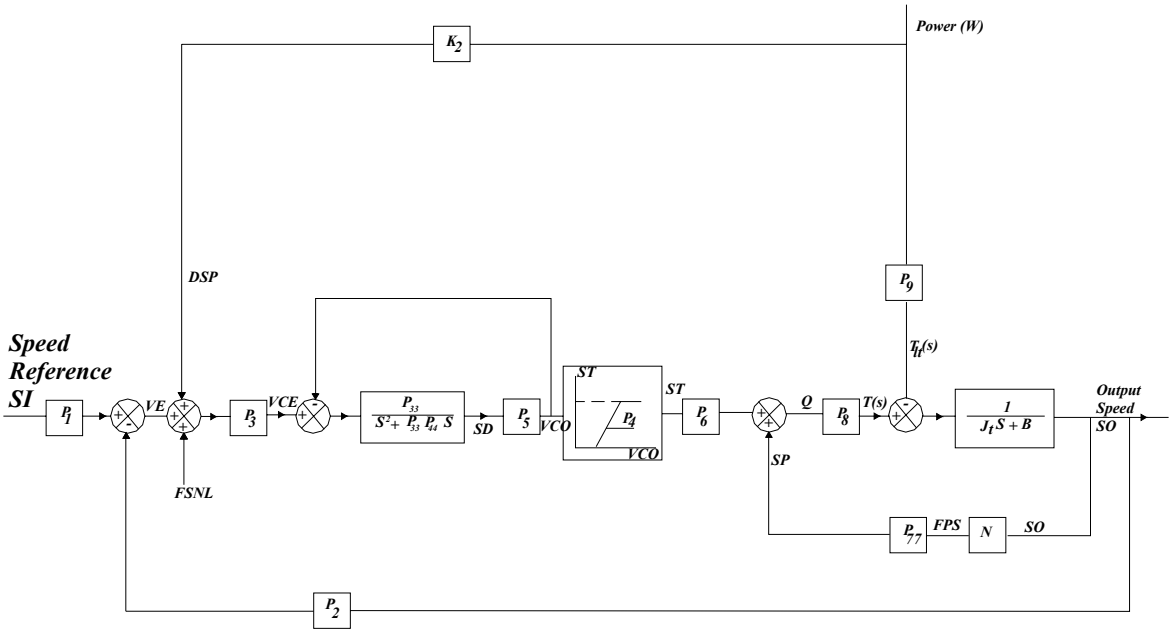

Figure(16):Block Diagram for Speed Control System.

3.4. The Numerical Integration Method:

3.4.1. Modified Euler's Method:

The modified Euler method is used as the numerical integration routine in modeling our system, such method has proved to give a good accuracy compared to the other difficult and complicated methods such as Runge-Kutte and the Predictor Corrector methods. The consideration of the linear system model in this study arises from three main reasons, the first is to check the accuracy of the numerical integration routine against the analytical solution of the system, the second reason is to find some initial estimate for the unknown parameter, the power amplifier gain (P_3), finally the system model will serve as a means for predicting the effects of parameters variations on the system performance in both linear and nonlinear. A better approximation than one-step Euler method is to use the mean value of the function derivatives at both ends of the time interval as shown in Figure (17), so the formula for the first integrator becomes:

$$D(I+1) = D(I) + \frac{DT}{2}(AC(I) + AC(I+1)) \quad \ldots(26)$$

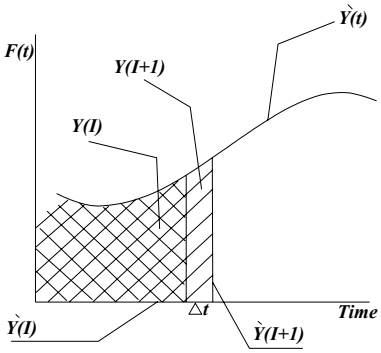

Figure(17): Graphical Representation for Euler Method.

3.4.2. Error Analysis:

For any numerical method of integration, there are mainly two sources of error which should be taken into consideration: truncation error which depends upon the number of terms of Taylor's polynomial used, and a rounding error which depends on the number of iterations carried out, and also upon whether single or double precision is used with the computer (Philips, G.M., 1973). The truncation error for modified Euler's method can be found as:

$$\varepsilon(t_{I+1}) = -\frac{h^3}{12}Y'''(t_I) - \frac{h^4}{24}Y'''(t_I) - \ldots.. \quad \ldots(27)$$

And the total error over n intervals is:

$$\varepsilon(T) = \sum -(\frac{h^3}{12}Y'''(t_I) + \frac{h^4}{24}Y'''(t_I) + \ldots) \quad \ldots(28)$$

The negative sign indicate that the values of any function calculated by this method are greater than the values given by Taylor's expansion.

4. Effect of Parameters Variations on Linear System Response:

The digital model for the linear system was used to study the different effects of variation in system parameters on its performance, assuming linear operations in two cases, at zero load and with load 10 MW.

4.1. Linear System at Zero load:

When changing the power amplifier gain (P_3) around its selected value (1.034) while all the other parameters are kept at their nominal values, different speed responses can be obtained as shown in Figure (18), from this Figure it is noticeable that the system steady state error increases at both higher and lower values for (P_3). The effect of changing (P_3) on the VCE voltage, fuel consumption are shown in Figure (19a,b), respectively. The similarity between the responses in the two figures is clearly noticeable; this is due to the fact that each of these two variables is a linear function of the other. It can also be seen that the two response of each of these variables increase as (P_3) increases.

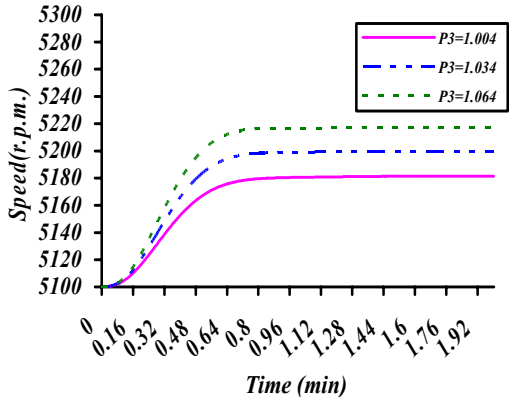

Figure(18):Effect of Changing P_3 on Turbine Speed for Linear System without Load

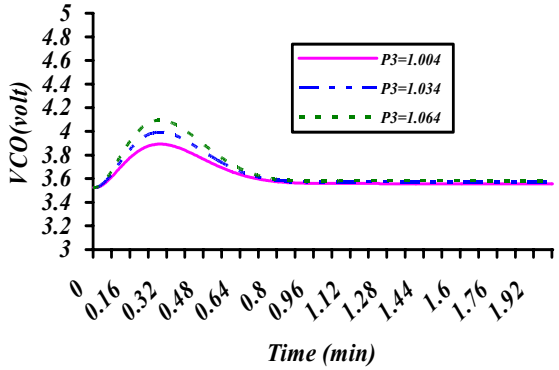

(A)

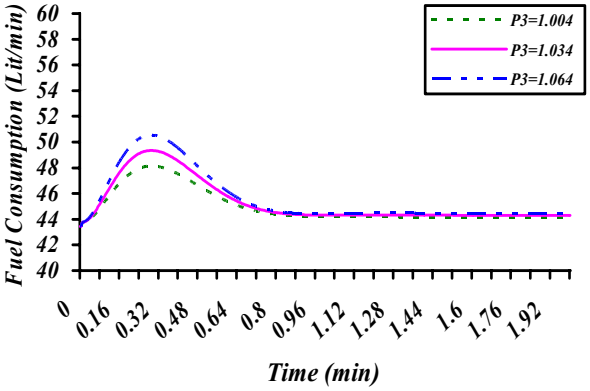

(B)

Figure(19): Effect of Changing P_3 on VCE and Fuel Consumption for Linear System without Load.

As mentioned above, parameter (P_8) is a measure of the thermal cycle efficiency which in turn depends on the electrical load connected to the unit generator. When changing the cycle efficiency around its estimated value (8.5%) which means (P_8=108.22), while all the other parameters are kept at their nominal values, the turbine speed will change as shown in Figure (20), in this figure three responses are shown, one at the nominal value and the two responses obtained at a higher and lower values for (P_8). It is clear that the system steady state error is greatly affected by any change in the cycle efficiency. The effect changing this parameter on the VCE and fuel consumption are also shown in Figures (21a,b) respectively. From these figures it can be noticed that as the cycle efficiency increases, the VCE voltage decreases and consequently the value of the fuel consumption decreases.

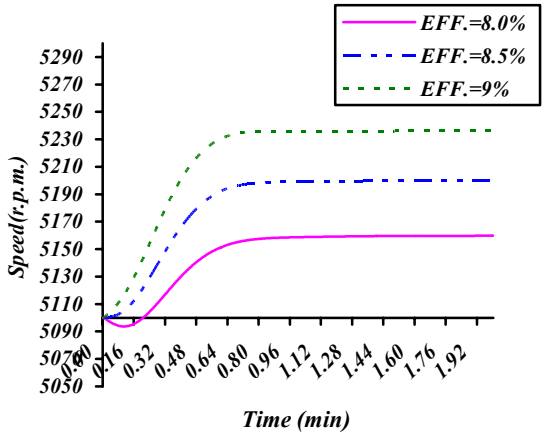

Figure(20):Effect of Changing Efficiency on Turbine Speed for Linear System without Load.

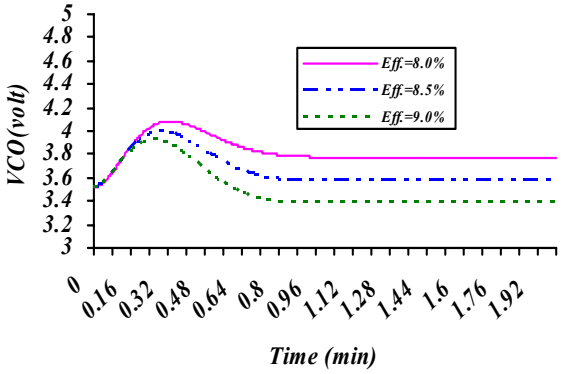

(A)

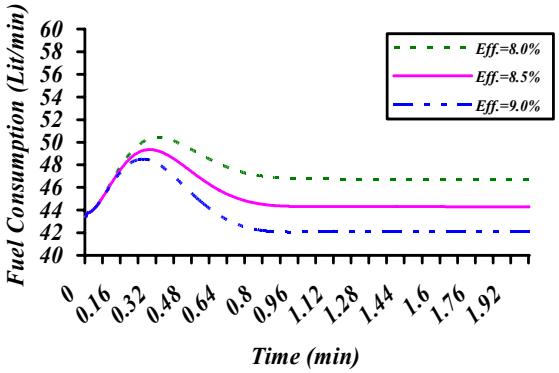

(B)

Figure(21): Effect of Changing Efficiency on VCE and Fuel Consumption for Linear System without Load.

4.2.Linear System with load 10 MW:

The effect of applied load on the performance of the linear system model can also be examined by adding the required load value and the corresponding "Digital Set Point" to the program, since the unit operating in the range (0-20) MW, mean value of 10 MW was chosen for this study. This leads to the only four changes, W=10, DSP=2.0, P8=318.34 and the initial value of fuel consumption (Q)=79.6, all the other parameters were kept at their nominal values and the effect of small variations in parameters (P_3) and (P_8) on the system performance were examined, by changing the value of (P_3) around its selected value (P_3=1.11) different responses for the change in the turbine speed can be obtained as shown in Figure (22). It can be seen that both of the peak over shoot and the steady state error of the speed response are largely affected by small changes in the value of this parameter, the drop in the speed at the initial time is also noticeable in all responses. The effect of changing (P_3) on the VCE voltage, and the fuel consumption are shown in Figures(23a, b) for the linear system with load 10 MW, it is clear from these figures that the oscillation in the response tends to increases with the increase of the power amplifier gain (P_3).

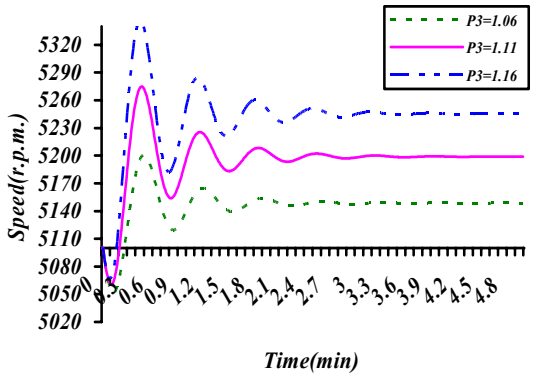

Figure(22):Effect of Changing P_3 on Turbine Speed for Linear System with Load 10 MW.

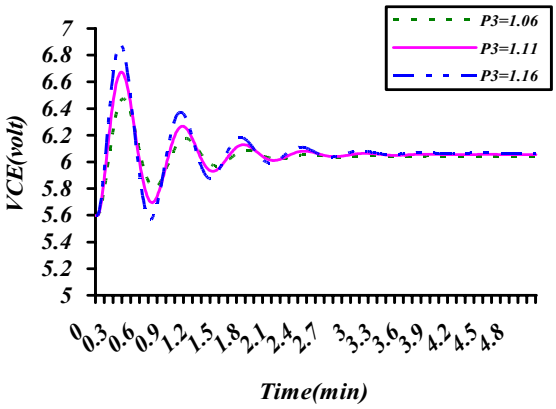

(A)

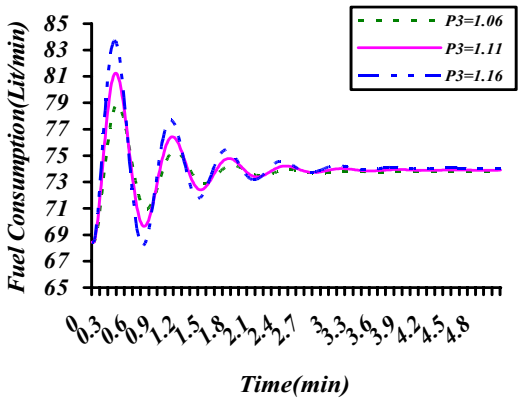

(B)

Figure(23): Effect of Changing P_3 on VCE and Fuel Consumption for Linear System with Load 10MW.

When load 10 MW is connected to the unit consequently P_8=318.294, assuming small deviations for the cycle efficiency around this value, different step responses for the turbine speed can be obtained as shown in Figure (24), from this figure, it can be noticed that the turbine speed is largely affected by any change in this parameter, where the step response is shifted upward with the increase in the cycle efficiency. The effect of small changes in this parameter on the VCE voltage, and fuel consumption are also shown in Figures (25a, b), respectively. It is clearly noticeable, in these figures that any increase in the cycle efficiency will decrease the value of the VCE voltage and consequently the values of the fuel consumption.

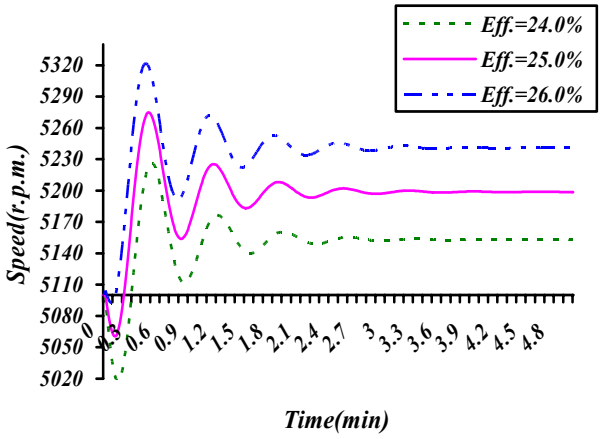

Figure(24): Effect of Changing Efficiency on Turbine Speed for Linear System with Load 10MW.

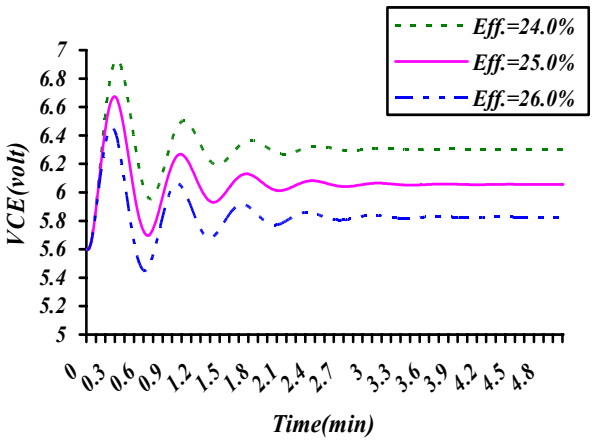

(A)

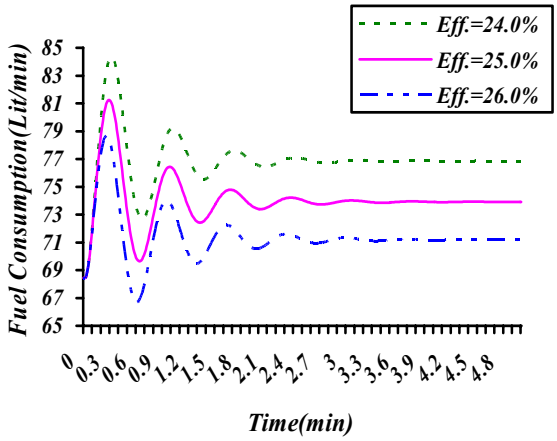

(B)

Figure(25): Effect of Changing Efficiency on Fuel Consumption for Linear System with Load 10 MW.

5. Analytical Solution:

In order to get a more general solution for the speed control system in its linear form and to check the accuracy of the integration routine used in the digital model. The system transfer function is obtained from the linearized system block diagram in two cases, at zero load and with load applied. In each cases, the system step response, the steady state error and the system stability are discussed.

5.1. Transfer Function at Zero Load:

Figure(16) shows the general block diagram for speed control system. Applying the basic reduction formula of feedback control without taken into consideration the load, such block diagram is reduced step by step to get the transfer function as:

$$\frac{SO(s)}{SI(s)} = \frac{P_1K_1 + K_1FSNL/SI(s)}{(s^2 + P_{33}P_{44}s + P_{33}P_5)(s + T_m(P_{10} - P_7P_8)) + P_2K_1} \quad \ldots(29)$$

When the speed of the unit is assumed to be changed instantaneously to a new value R(r.p.m), so it can be written as:

$$SI(s)=R/s \quad \ldots(30)$$

Thus, the system transfer function at zero load becomes:

$$SO(s) = \frac{P_1K_1R/s + K_1FSNL}{(s^2 + P_{33}P_{44}s + P_{33}P_5)(s + T_m(P_{10} - P_7P_8)) + P_2K_1} \quad \ldots(31)$$

By using the partial fraction and the Laplace transform, to get the analytical solution:

$$SO(t) = 4492.476 - 2283.53e^{-4.9905t} - 2208.94e^{-50812t}\cos(6.3788t) - 3546.1626e^{-5.0812t}\sin(6.3788t) \quad \ldots(32)$$

In order to compare between the linear model and the analytical solution, a complete list of the result are given in Table (1).

Table(1):Values of Model and Analytical Step Responses at zero Load

Time	Speed(Model)	Speed(Analytical)	Time	Speed(Model)	Speed(Analytical)
.100	5104.35800	5107.42900	1.100	5199.21900	5197.99700
.200	5120.57100	5123.95900	1.200	5199.38200	5198.13700
.300	5143.91800	5145.97900	1.300	5199.55200	5198.29900
.400	5166.04300	5166.58100	1.400	5199.69300	5198.44000
.500	5182.22900	5181.74300	1.500	5199.79000	5198.54100
.600	5191.86200	5190.89600	1.600	5199.84400	5198.60000
.700	5196.55900	5195.44100	1.700	5199.87100	5198.62800
.800	5198.38700	5197.24300	1.800	5199.88200	5198.64000
.900	5198.93700	5197.77500	1.900	5199.88200	5198.64400
1.000	5199.09400	5197.90400	2.000	5199.88200	5198.64500

5.2. Transfer Function at Load Applied:

When considering the load applied by the unit generator on the performance of the speed control system, the general block diagram for the control system as shown in ***Figure(16)***. It was reduced step by step to get the transfer function as follows:

$$\frac{SO(s)}{SI(s)} = \frac{P_1K_1 + (K_1K_2 - Tm\,P_9\,s^2 + P_{33}\,P_{44}s + P_{33}\,P_5)\frac{W}{SI(s)} + K_1\frac{FSNL}{SI(s)}}{(s^2 + P_{33}P_{44}s + P_{33}P_5)(s + T_m(P_{10} - P_7P_8)) + P_2K_1} \quad \ldots(33)$$

The system output speed with load applied can be written from ***equation (31)*** as :

$$SO(s) = \frac{P_1K_1SI - Tm\,P_9(s^2 + P_{33}\,P_{44}s + P_{33}\,P_5)W + K_1(DSP + FSNL)}{(s^2 + P_{33}P_{44}s + P_{33}P_5)(s + T_m(P_{10} - P_7P_8)) + P_2K_1} \quad \ldots(34)$$

For the speed change from ***0 to R=5100 r.p.m,*** also the above equation becomes:

$$SO(t) = 4907.244 + 544.62e^{-12.03851t} - 12945.25e^{-1.541t}\cos(8.7923t) - 20323.346e^{-1.541t}\sin(8.792t) \quad \ldots(35)$$

In order to compare between the linear model with load 10 MW and the analytical solution a complete list of the result are given in Table (2)

Table (2): Values of Model and Analytical Step Responses at Load 10 MW.

Time	Speed(Model)	Speed(Analytical)	Time	Speed(Model)	Speed(Analytical)
.200	5088.47400	5096.85800	2.800	5197.76900	5197.66800
.400	5253.43200	5192.23700	3.000	5197.58800	5195.25800
.600	5237.21000	5248.85500	3.200	5199.85500	5195.70200
.800	5155.18700	5183.75000	3.400	5199.14100	5196.88100
1.000	5193.57500	5171.20200	3.600	5198.16300	5196.31800
1.200	5224.48300	5209.81200	3.800	5198.90400	5195.83600
1.400	5192.49300	5206.00200	4.000	5199.17000	5196.27200
1.600	5187.13500	5186.19900	4.200	5198.67100	5196.41300
1.800	5206.47800	5193.68600	4.400	5198.70400	5196.13900
2.000	5202.45800	5202.32600	4.600	5198.96300	5196.13800
2.200	5193.36500	5195.91500	4.800	5198.85300	5196.28600
2.400	5198.81600	5193.00700	5.000	5198.75100	5196.24600
2.600	5201.81300	5197.26600			

5.2. System Steady State Error:

The steady state error indicates the error between the actual output and the desired output as the time goes to infinity. The steady state error is a measure of the control system accuracy (Raven, 1978). In our system, it has critical importance, since any change in the turbine speed will produce a change in the unit generator speed and consequently will cause a change in the electrical network frequently.

5.2.1 Steady State Error at Zero Load:

The error signal can be written as

$$VE = SI(s) - H(s)SO(s) \quad \ldots(36)$$

Substituting ***equation (31)*** in ***equation (36)***, to get:

$$VE = \frac{SI(s)((s^2 + P_{33}P_{44}s + P_{33}P_5)(s + T_m(P_{10} - P_7P_8))) - K_1\,FSNL}{(s^2 + P_{33}P_{44}s + P_{33}P_5)(s + T_m(P_{10} - P_7P_8)) + P_2K_1} \quad \ldots(37)$$

When using the final value theorem, the steady state error can be obtained as:

$$VE(s)_{ss} = \lim_{s\to 0} sVE(s) \quad \ldots(38)$$

If we assume unit step input $SI(s) = 1/s$ and substitute the numerical value of the system parameters at zero load, the steady state error can be calculated using the expression:

$$VE_{ss} = \frac{T_mP_{33}P_5(P_{10} - P_7P_8)}{T_mP_{33}P_5(P_{10} - P_7P_8) + P_2K_1} \quad \ldots(39)$$

To get:

$$VE_{ss} = 0.0135 \quad \ldots(40)$$

For speed change from 5100-5200 r.p.m, in order to compare the digital model with it, which yield:

$$VE_{ss} = 1.35\ r.p.m.$$

From the results of the digital model given in Table (1), the value of the steady state error can be found as:

$$VE_{ss} = 5200 - 5198.645 = 1.355\ r.p.m.$$

Which is quite close to the calculated value.

5.2.2 Steady State Error with Load:

Since the output speed is :

$$SO(s) = \frac{P_1 K_1 SI(s) - Tm\ P_9 (s^2 + P_{33} P_{44} s + P_{33} P_5) W + K_1 (FSNL + DSP)}{(s^2 + P_{33} P_{44} s + P_{33} P_5)(s + T_m (P_{10} - P_7 P_8)) + P_2 K_1} \quad \ldots(41)$$

Substituting into ***equation (36)***, to get:

$$VE = \frac{SI(s)(s^2 + P_{33} P_{44} s + P_{33} P_5)(s + T_m (P_{10} - P_7 P_8))}{(s^2 + P_{33} P_{44} s + P_{33} P_5)(s + T_m (P_{10} - P_7 P_8)) + K_1 P_2} + \frac{(T_m P_9 (s^2 + P_{33} P_{44} s + P_{33} P_5) - K_1 K_2) W - K_1 (FSNL + DSP)}{(s^2 + P_{33} P_{44} s + P_{33} P_5)(s + T_m (P_{10} - P_7 P_8)) + K_1 P_2} \quad \ldots(42)$$

By assuming unit step input as before, and substituting the numerical values of the system parameters with load ***10 MW***. The steady state error can be calculated from the expression:

$$VE_{ss} = \frac{P_{33} P_5 T_m (P_{10} - P_7 P_8)}{P_{33} P_5 T_m (P_{10} - P_7 P_8) + K_1 P_2} \quad \ldots(43)$$

This gives,

$$VE_{ss} = 0.03813 \quad \ldots(44)$$

For speed change from ***5100 to 5200 r.p.m.*** this value becomes

$$VE_{ss} = 3.81\ r.p.m.$$

Comparing it with the numerical values given in Table (2) where the steady state error is:

$$VE_{ss} = 5200 - 5196.246 = 3.754\ r.p.m.$$

Which is close to the value obtained from equation (44)

5.3. Stability of the Linear System:

A very important characteristics for any control system whose response is bounded for every bounded input. That is, if the system is subjected to input or disturbance signal with a certain magnitude and the response is bounded in magnitude, the system is said to be stable (Drof, 1980). The Routh criterion is a mathematical method used to determine the stability (or instability) of linear control systems, it involves setting up an array of numbers based on the coefficients of the systems characteristic equation, for every change in sign in the first column of the array, a root of the characteristic equation exists with positive real part. This is in turn would indicate unstable system. In this research according to the characteristic equation (31) at zero loads with the Routh criteria, it is clear that there is no change in signs on the first column of the characteristic equation, which means that the system is stable. The same procedure can be used for load 10 MW there is no change in signs of the first column of the characteristic equation (33) which mean that the system with load also is stable.

6. Digital Model for the Actual Speed Control System:

The digital model of the nonlinear speed control system is based on the same numerical integration routine used for the linear system model in the above sections with only introducing the system nonlinearities as given the system block diagram, since the two non-linearities existed in our system, the dead zone and the saturation are not time dependent nonlinearities, so their addition to the system model will not affect the numerical integration, but will only put some limitations on the model variables. The representation of the system non-linearities in this model can be considered as three regions:

i) Dead zone for ***VCO≤4***, where the value of the output pump stroke ***(ST)*** and the fuel consumption ***(Q)*** will always be equal to zero for all ***input signal ≤4***.

ii) Linear region for ***4<VCO<18*** where the value of the fuel pump stroke ***(ST)*** can be obtained as a linear function of the input voltage **(VCO)** as

$$ST = 0.714 * VCO - 2.856 \quad \ldots(45)$$

iii) Saturation limit for ***VCO≥18,*** where the input voltage reaches ***18 volts,*** the servo valve stroke will reach its maximum value of ***10 mm*** and remains at this value whatever the input voltage increases.

7. Comparison between the Digital Model Results and the Actual System Performance:

In order to examine the validity of the digital model, which we have already to simulate the actual nonlinear system, it is necessary to compare the results obtained from this model at a certain working condition with the results obtained from the actual system at the same working condition. In the data given by the manufacture, there were some available values for the system variables at steady state working condition with zero load and normal running speed of 5100 r.p.m.. So, it was reasonable to run the digital model at zero load condition for speed change from 0 to 5100 r.p.m., then to compare the results obtained at the steady state condition with the given by the manufacture. Table (3) shows such comparison, four variables are used in this comparison, the VCE, the fuel stroke (ST), the fuel consumption (Q), and the turbine speed. It is clear that the value values estimated by the system digital model are very close to the values given by the manufacturer, which proves the validity of the digital model in simulating the actual speed control system with high accuracy.

Table (3): A comparison between The Digital Model Results and The Manufacturer Data.

System Variable	Model Results	Manufacturer Data
Electronic Control Voltage (VCE)	7.499 volts	7.5 volts
Fuel Pump Stroke (ST)	2.498 mm	2.5 mm
Fuel Consumption	43.45 lit/min	43.5 lit/min
Turbine Speed	5099.96 r.p.m.	5100 r.p.m.

8. Effects of Parameters Variation using The System Digital Model:

8.1. Effect of Changing (P_1)

The value of parameter ***(P_1)*** was changed by ± ***1%*** of its nominal value ***(0.0049)*** and the system digital model was run at each of these values. Typical responses for the turbine speed at these values are shown in ***Figure (26)*** where it can be seen that as the value of ***P_1*** increases, turbine speed increases and the amount of steady state error increases in both cases.

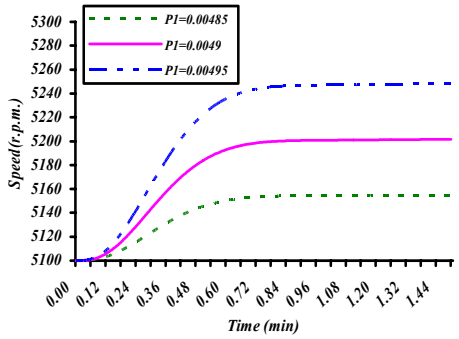

Figure(26):Effect of Changing P_1 on Turbine Speed for Non-Linear System without Load.

8.2. Effect of changing P_2:

When the value of the magnetic pick-up gain (P_2) is varied by ± 1% of its nominal value, another set of responses can be obtained as given in Figure(27), by comparing Figures(26) and (27) we notice that the change in P_2 has an opposite effect to the change in P_1, since the value of the turbine speed decreases with the increases in parameter P_2. the reason for this is for P_2 being in the feedback path where the values are subtracted from the feed forward path.

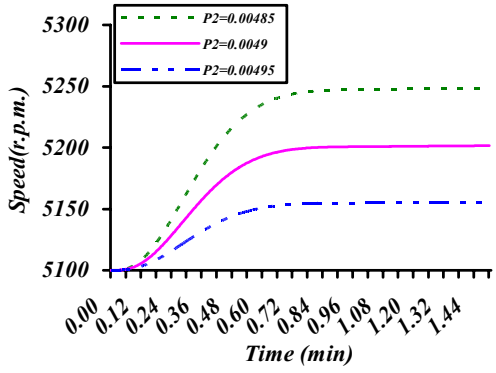

Figure (27): Effect of Changing P_2 on Turbine Speed for Non-Linear System without Load.

8.3.Effect of changing P_4

When the value of parameter P_4 is changed by ±5% of its nominal value, different responses for the turbine speed can be obtained as shown in Figure (28) from these responses, it is clear that the

system steady state error is largely affected by the changing in this parameter, we also notice that for low value of P_4 the output speed tends to drop below the normal running speed.

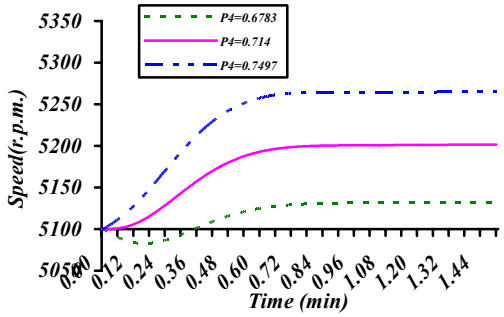

Figure(28): Effect of Changing P_4 on Turbine Speed for Non-Linear System without Load.

8.4.Effect of changing in P_{33} and P_{44}:

Each of the two parameters P_{33} and P_{44}, which represent the feed forward gain of the hydraulic servo valve and the feedback gain, respectively, is changed by about ±25% of the nominal value. The system responses at these new values are plotted in Figure(29a, b), respectively, in these two figures, it is clear that even with such large deviations the system performance is slightly affected by these two parameters.

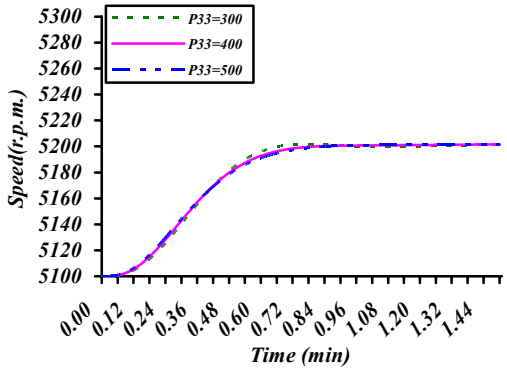

(A)

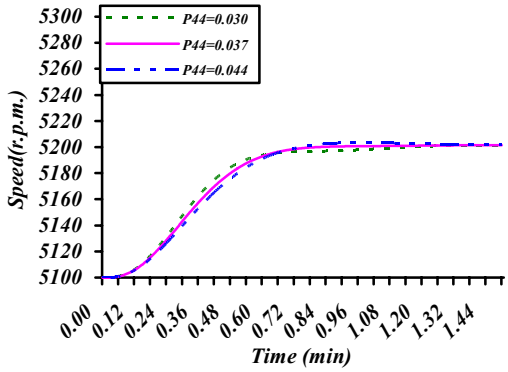

(B)

Figure(29): Effect of Changing P_{33} and P_{44} on Turbine Speed for Non-Linear System without Load.

8.5. Effect of changing P_5

The gain of the ***LVDT (P_5)*** was also changed by ***±5%*** from its nominal value and different responses for the turbine speed were obtained as plotted in ***Figure (30).*** This figure shows clearly that the change in this parameter has no effect on the system steady state error, but it has some slight effect

on the turbine speed at the early time of the response. A drop in the speed below the normal running value can also observed where P_5 is decreased.

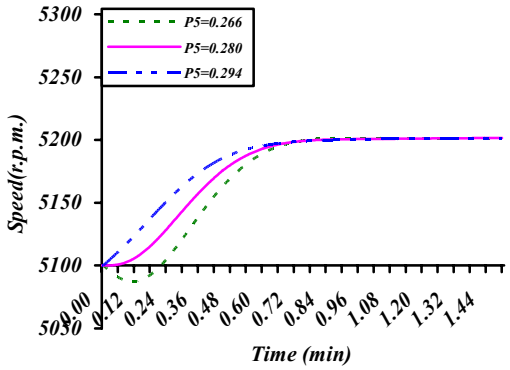

Figure(30): Effect of Changing P_5 on Turbine Speed for Non-Linear System without Load.

8.6. Effect of Changing T_m and P_{10}:

The nominal value for each of these parameters were changed by ±5% and the obtained turbine speeds in each case are plotted in Figures (31 a, b), respectively. It can be concluded from these two figures that the change in ™ has very small effect on the turbine speed and the system steady state error, while the changing in parameter P_{10} affects both the turbine speed and the system steady state error when it is either increased or decreased from its nominal value.

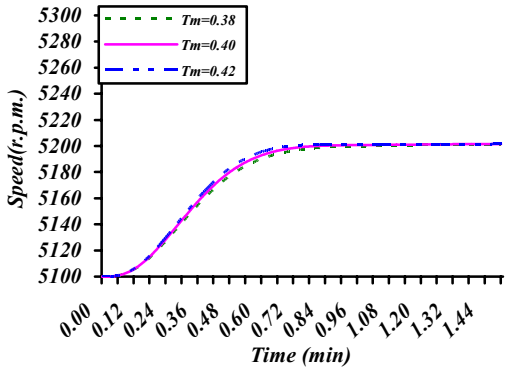

(A)

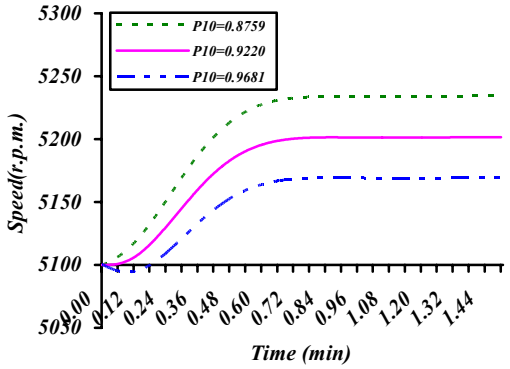

(B)

Figure (31): Effect of Changing T_m and P_{10} on Turbine Speed for Non-Linear System without Load.

8.7. Effect of Changing FSNL

Finally, the value of the full speed no load voltage was changed by ***±5%*** of its nominal value, and the corresponding system responses were plotted as shown in ***Figure(32)***, this figure shows clearly that the system response is very sensitive to any change in this parameter, as can be seen from larger value of the system steady state error occurred at both higher and lower values of this parameter.

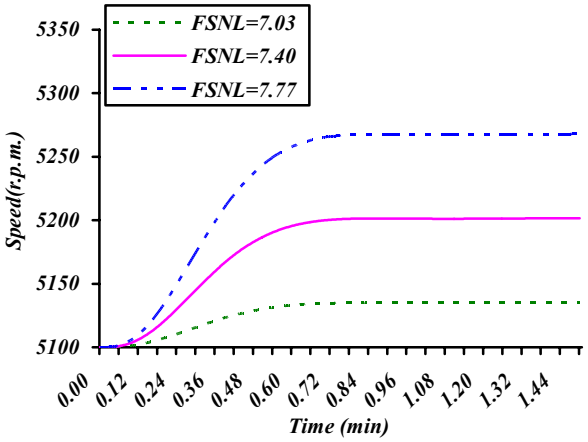

Figure(32): Effect of Changing FSNL on Turbine Speed for Non-Linear System without Load.

9. Effect of Parameters Variations at Different Load Condition:

Two of system parameters, the power amplifier gain P_3 and the cycle efficiency P_8 have been chosen to perform the comparison.

9.1. Zero Load Condition:

If parameter P_3 is changed by small value ±2% around its adjusted value (1.024) at zero load condition, different response for the system speed can be obtained as shown in Figure(33), from such response it is clear that the system steady state error increases with any change in parameter P_3 from the selected value. The effect of small change in P_3 on the unit fuel consumption is also shown in Figure(34), from this figure it can be concluded that the fuel consumption increases with the increase in P_3, also the maximum increase in the fuel consumption occurs at time equal 0.48min. The cycle efficiency P_8 was also changed by small deviation around its nominal value, and three step responses for the turbine speed were obtained at three different values of P_8 as given Figure(35). When examining the effect of same changes on the unit fuel consumption as given in Figure(36), it can be noticed that the fuel consumption decreases with the increase in the cycle efficiency, it is also clear that the maximum variation in the fuel consumptions occurs when steady state operation is reached.

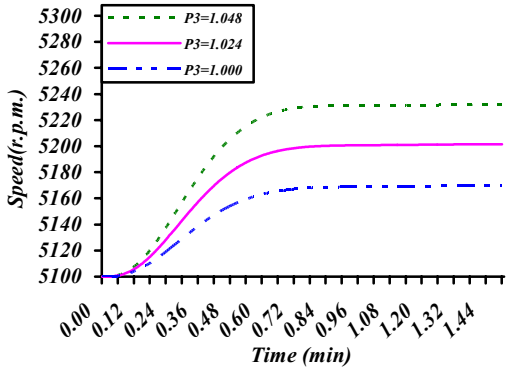

Figure(33): Effect of Changing P_3 on Turbine Speed for Non-Linear System without Load.

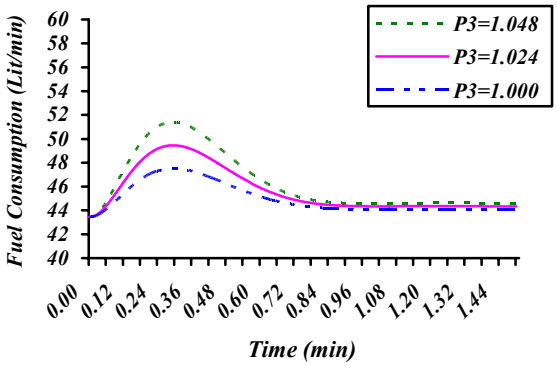

Figure(34): Effect of Changing P_3 on Fuel Consumption for Non-Linear System without Load.

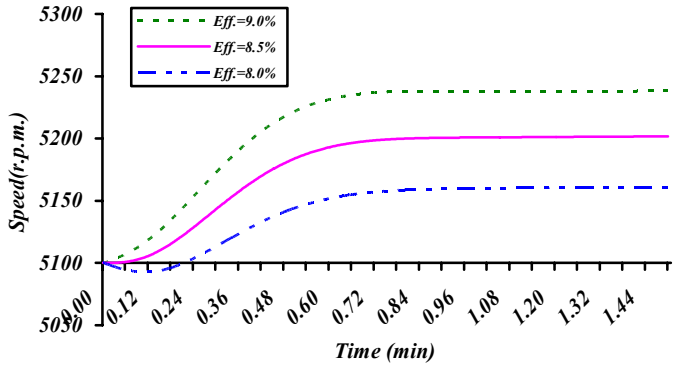

Figure(35): Effect of Changing Efficiency on Turbine Speed for Non-Linear System without Load.

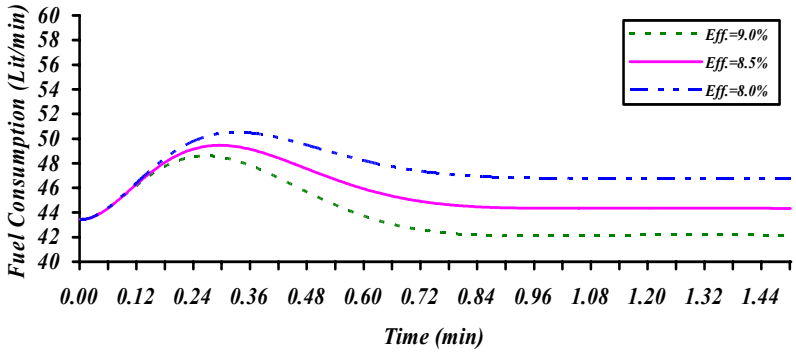

Figure(36): Effect of Changing Efficiency on Fuel Consumption for Non-Linear System without Load.

9.2.Full Load Condition (20MW):

For full load condition, the optimum value of P_3 was found to be (1.211), when this value is deviated by ±1% the turbine speed will affected as shown in Figure(37a), while the fuel consumption will be affected as given in Figure(37b). The first figure shows clearly that the system speed and its steady state error are changed with any change in parameter (P_3),we may notice that the oscillation in the system response tends to increase with the increase in the load, while the duration of the response becomes longer. As for the effects on the fuel consumption, we also notice that the values of fuel consumption at initial condition and at steady state error condition have increased with the increase in load, at the same time the effect of small deviations in P_3 is nearly negligible, as can be seen in Figure(37b). The cycle efficiency P_8 at load (20 MW) is 28%. When this value is deviated by ±2% we can get different responses for the turbine speed and for the fuel consumption as shown in Figures(38a, b). These figures show clearly that the turbine speed and the fuel consumption are

sensitive for small changes in the cycle efficiency, but with different reactions, where the turbine speed increases with any increase in the efficiency while the fuel consumption decreases.

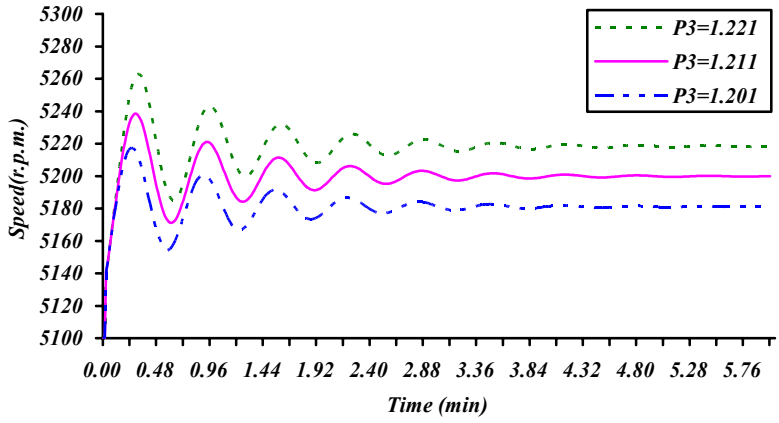

(A)

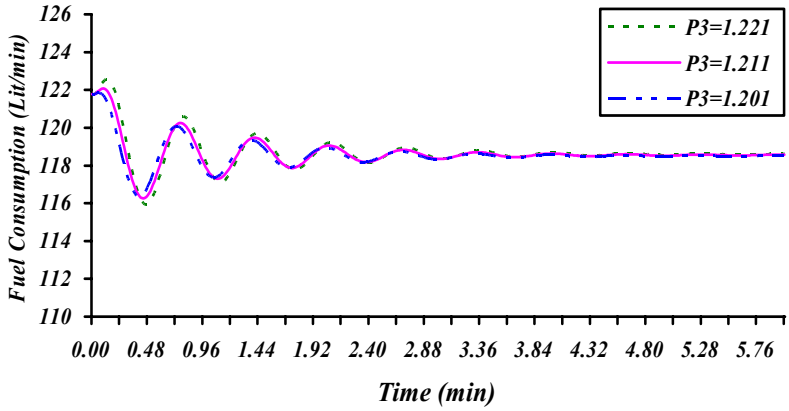

(B)

Figure(37): Effect of Changing P_3 on Speed Turbine and Fuel Consumption for Non-linear System with Load 20MW.

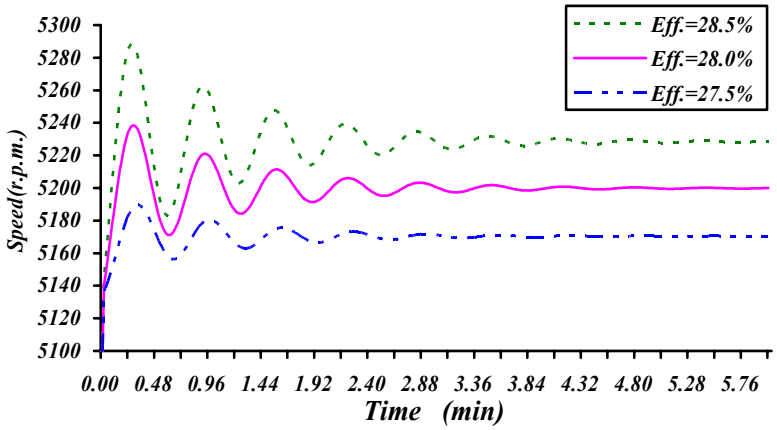

(A)

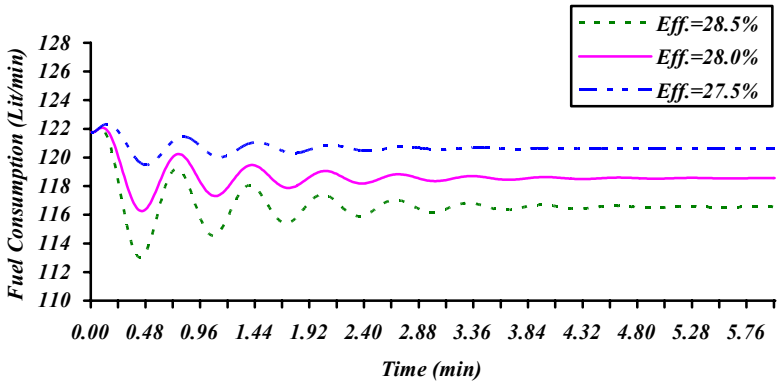

(B)

Figure(38): Effect of Changing Efficiency on Speed Turbine and Fuel Consumption for Non-linear System with Load 20MW.

10. Conclusions

This research has shown clearly that the analysis and study of gas turbine control system is not an easy task, because of the wide interaction among the system components and also because of the performance limitations imposed upon the system during its actual operation. At the same time, digital simulation technique has proved to be an efficient tool treating such control system. The system digital model was found to be useful for the optimization process of the system unknown parameters, as well as, in predicting the various effects of parameters variations on the system performance, such as the power amplifier gain and the cycle efficiency are having large effects on the speed of the gas turbine, while some other parameters, such as the gear ratio between the turbine and the fuel pump, have very small effect on the system performance. The digital model has shown clearly that the load connected to the generating unit is a major factor in determining the performance of the speed control system, in both the magnitude and the duration of the transient response for the turbine speed, which agrees with the actual working conditions. The accuracy of the digital model has proved to be quite sufficient when compared with the results obtained from the analytical solution of the linearized system transfer function. System nonlinearities, caused by the performance limitations for some of the system components, have shown noticeable effects in improving the speed characteristic of the gas turbine and helped to overcome the major defects in the system transient response.

References

"Mark I and II Speedtronic Control System Manual"

Abraham, G.A., 1969. "The Advancement of Control with Modern Gas Turbine", Proc. Inst. Mech. Engr. Vol.183, Pt3N, PP.138-149.

Bammert, K. and Kret, G., 1971. "Dynamic Behavior and Control of Signal Shaft Close-Cycle Gas Turbine", Trans. Of ASME, Journal of Power Engineering, PP.447-453, October.

Centeno, P., et. al., 2002. "Review of Gas Turbine Model for Power System Stability Studies", http:\\ www.368-centeno, keyword: Stability Studies, Dynamic Models, Gas Turbines.

Cohen, H., Rogers, G.F.C., Saravanamuttoo, H.I.H., 1992."Gas Turbine Theroy", Longman Scientific and Technical.

Dent, J. R., 1970. "The Electronic Control of automotive Gas Turbine Engine", ASME Paper 70-GT 119.

Drof, R. C., 1980."Modern Control System", Addison Wesley.

Ederven, J., 1971."Control System for Medium Size Gas Turbine", SAE Paper 710549.
Gerald, C. F., 1973."Applied Numerical Analysis", Addison Wesley.
Gill, K. F., 1978."System Modeling and Control", Edward Arnold Ltd.
Harrison, H.I., Bollinger, J.G., 1969." Introduction to Automatic Control", Intertext Books.
Hogg, B. H., 1981."Modeling of Dynamical System", Vol.2, Peter Peregrinus Ltd.
Japan's Staff Report, 1982. "Japan's Utilities Turn to Giga watt Combined Cycle Plants", Modern Power System, Vol.2, No.3, PP.33-40.
Jerald, G. G., 1973. "Application of Operational Amplifier", McGraw Hill.
Loft, A., 1968. "Speedtronic Tomorrow's Analog and Digital Gas Turbine Control System", IEEE 15th Annual Petroleum and Chemistry, Paper No. PCI-68-16, September.
Mantzaris, J., and Vournas, C., 2007. "Modeling and Stability of a Single shaft Combined Cycle Power Plant", Inst. Journal of Thermodynamic, Vol.10, No.2, PP.71-78.
McArthur, M. J., Charles, J., 1969. "Recent Development in the Control of Industrial Gas Turbine", Proc. Inst. Mech. Engg., Vol.83, Pt3N, PP.128-137.
Ogata, K., 2002. "Modern Control Engineering", Prentice Hall of India Ltd.
Openshow, F., and Estrine, K., 1976. "Control of a Gas Turbine HTGR", ASME Paper 76-GT-97.
Philips, G. M., 1973. "Theory and Application of Numerical Analysis", Academic Press.
Raven, F. H., 1978. "Automatic Control Engineering", McGraw Hill.
Richard, T. C., 1981. "Gas Turbine Engineering Application, Cycles and Characteristics", the Macmillan Press Ltd,
Rowen, W. I., 1983. "Simplified Mathematical Representation of Heavy Duty Gas Turbines", Transactions of the ASME Journal of Engineering for Power, Vol.105, PP.865-870.
Rowen, W. I., 1997. "Simplified Mathematical Representation of Single Shaft Gas Turbines in Mechanical Drive Service" Proc. The International Gas Turbine and Aeroengine Congress and Exposition, Cologne, Germany,
]Rowen, W.I., 1988."Operating Characteristic of Heavy Duty Gas Turbines in Utility Service", Proc. The Gas Turbine and Aero engine Congress, Amsterdam, the Netherlands.
Sadlery, A. and Tweedy, S., 1963. "The Electronic Control of Gas Turbines", Journal of Royal Aeronautical Society, Vol.69, No.655, Pp. 429-447.
Silva, V. R. E., and Khatib, W., 2007. "Control System Design for Gas Turbine Engine using Evolutionary Computing for Multidisciplinary Optimization", Revista. Control and Automatic, Vol.18, No.4, November.
Trandle, B., 1979. "Egatral Electronic Control System for Gas Turbine", Brown Bovery Rev., Vol.66, Part 2, PP.113-119.
Wilson, K.G., 1979. "Gas Turbine Control", Engineering, Vol.219, PP.1129-1131.
Wolzer, P., and Meler, P., 1979. "An Electronically Controlled Automotive Gas Turbine", ASME Paper 79-GT-74,